MODELING PERSISTENT CELL MOVEMENT IN ABSENCE OF EXTERNAL SIGNAL WITH THE CELLULAR POTTS MODEL

DON CHANUKA UDAYANGA KARAWITA

A dissertation submitted in partial fulfilment of the requirements for the Bachelor of Science Special Degree in computational Physics

Of the

University of Colombo, Sri Lanka

FEBRUARY 2018

DECLARATION

I certify that this dissertation does not incorporate without acknowledgement, any material previously submitted for a Degree or Diploma in any university and to the best of my knowledge and belief it does not contain any material previously published or written or oral communicated by other person except where due reference is made in the text.

.....

Your name

ACKNOWLEDGEMENT

It is with great pleasure that I express my sincere gratitude to the project supervisor Dr. Siyath Gunawardena of the Department of Physics, University of Colombo for allowing me to work on one of his interesting projects. This would not have been a success if not for his constant inspiration, monitoring, guidance, invaluable feedback and suggestions throughout the project.

Last but not least, a special thank goes to my family members and all my colleagues for the moral support and help to carry through difficult times.

ABSTRACT

The Cellular Potts Model (CPM) is a stochastic method for modeling and simulating collective cell behavior in biology. It has been applied to many applications in biology such as blood vessel growth, somitogenesis, wound healing and tumor growth. Cell movement can be happened as a consequence of membrane fluctuations due to cell-cell interactions, or as a response to an external chemotactic gradient or without external signal. In this project, we considers about cell movement due to absence of external signal. Cellular Potts model is used combination with an equal constant force and random direction applied over each cell. This promotes a uniform cell motion in a given direction during a certain time interval, after which the movement direction changes. The dynamics of the direction is coupled to a first order autoregressive process. Statistical quantities, such as the mean-squared displacement associated to these self-propelled cells has analyzed. This model emulates many properties observed in different real biological experiments. As well as behavior of the simulation corresponds to the theoretical behavior.

TABLE OF CONTENTS

LIST OF FIGURES

LIST OF TABLES

ABBREVIATIONS

MCS	–	Monte Carlo time Steps
CPM	–	Cellular Potts Model
DAH	–	Differential Adhesion Hypothesis
MSD	–	Mean Square Displacement
MCMC	–	Markov Chain Monte Carlo

1 INTRODUCTION

1.1 Overview

Modelling biological systems is important task of systems biology and mathematical biology. Biological problems have been studied using mathematics for hundreds of years. But much of these studied problems have been restricted to ecological modeling (i.e. population dynamics). Models of morphogenesis, that is the study of the biological processes that govern the development of an organism's shape, are also widely studied models within mathematical biology.

There are different approaches to the modelling. One approach is whether its variables be continuous or discrete. Another approach is whether model be deterministic or stochastics. In deterministic models, all future states can be determined. Deference equations, Ordinary differential equations (ODEs), Partial Differential Equations (PDEs) are examples for deterministic models. Biological phenomena are difficult to predict with absolute certainty. Stochastic models reflect this uncertainty. Cellular Automata, Cellular Potts Model are example for stochastic models. Discrete models in mathematical biology are of interest because many biological structures are discrete by nature (e.g. cells in a tissue), and thus are most naturally modeled by a discrete model. In many cases it may be quite difficult to model these discrete structures using a continuum approach

In this project, our main task is to model persistent cell movement in absence of external signal. Since cellular Potts model is used to analyze biological process that involve adhesion and change in cell shape, CPM is suitable model for this task. Recent findings have shown that eukaryotic cells can exhibit persistent displacements across scales larger than cell size, even in the absence of external signals. Therefore Active cell movement is very important mechanism to study in system biology. Purpose of this project is discover characteristics of the active cell movement and check whether it is acceptable with real cell experiment.

1.2 Cellular Potts model

To model the cell sorting, Glazier and Graner developed their Cellular Potts Model (CPM) in 1992 (Graner and Glazier, 1992). This model takes the adhesion between the cells as a base for the rearrangement of cells, which is determined stochastically. CPM is modification of a large-Q Potts model. Although the model was developed to model biological cells it can also be used to model individual parts of a biological cell i.e. nucleus, plasma membrane and cytosol(Scianna and Preziosi, 2012). As well as CPM fall into category of agent based models (ABM).

This model is powerful and relatively easy to understand and is therefore used in a wide range of biological fields, including growth of blood vessels (Merks *et al.*, 2008), somitogenesis (Hester *et al.*, 2011), and wound healing (Scianna, 2015) and tumor growth(Szabó and Merks, 2013) . Depending on the problem one is facing, the model can be extended in various ways. For example, one may consider to add an extra component that takes the change of size of the perimeter (surface in 3D) of the membrane in the CPM into account.

The differential adhesion hypothesis (DAH) that is proposed by biologist Malcolm Steinberg in 1964 explains cell sorting and related cell rearrangements as progressions of motile and mutually adhesive cell populations toward configurations of minimal interfacial (adhesive) free energy. Many behavioral predictions based upon this hypothesis have been confirmed (Steinberg, 1975). According to the DAH hypothesis, cell sorting is a matter of minimizing free energy. CPM was originally designed to model this particular phenomenon.

Previous Simulations of cell sorting on a lattice either took cell to be a point like or use nonrealistic rules to describe topological changes. . The assumption of point like cell is dangerous to make, because the shape and size of a biological cell are nontrivial characteristics of a cell, and the fact that the cellular Potts model does not make these same assumptions is a strength of the model.

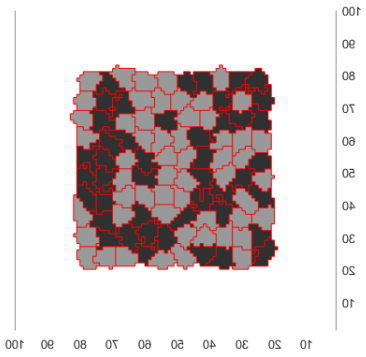

Figure 1-1 cell sorting at initial state

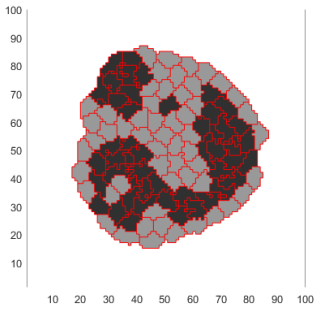

Figure 1-2 cell sorting at 50 MCS

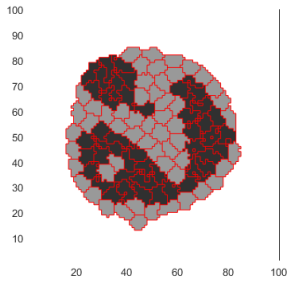

Figure 1 -1-3 cell sorting at 100 MCS

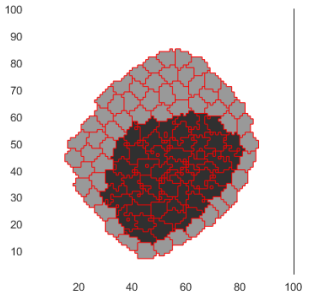

Figure 1 -1-4 cell sorting at 400 MCS

1.3 Cell migration

Cell migration is a basic cell function that underlies life. Cell migration is important for embryogenesis, immune surveillance and wound healing all require the orchestrated movement of cells in particular directions to specific locations. Cells often migrate in response to specific external signals, including chemical signals and mechanical signals. Errors during this process have serious consequences, including intellectual disability, vascular disease, tumor formation and metastasis. For example, many congenital defects in brain development leading to mental disorders can be attributed to defects in neuronal migration. Cell migration is central to homeostatic processes, such as mounting an effective immune response and the repair of injured tissues. An understanding of the mechanism by which cells migrate may lead to the development of novel therapeutic strategies for controlling (example: invasive tumor cells). Especially in areas of biotechnology that focus on cellular transplantation and the manufacture of artificial tissues. Understanding migration presents a formidable intellectual challenge because it is the product of several complex, integrated processes that must be carefully regulated. Therefore Mathematical models and Computer simulations are essential for understanding cell migration(Jagt, Neumann and Schulp, 2007; Mak *et al.*, 2016).

In this project, it is developed a computer simulation for low and high density cell cultures in persistent cell movement when external signals are absent. For this purpose, it is used the CPM, which considers cell adhesion and deformation, to better describe cell-cell interactions. Directional propensity vector is introduced that consider active cell movement in the absence of external cues (Szabó *et al.*, 2010). In this sense, we link the polarization direction of the cell to an autoregressive process that changes the migration direction after some characteristic time τ. and study the dynamics of the resulting cell movements. We perform computer simulations for different parameter values and find that the dynamics of these in silico-cell movements resembles the behavior observed experimentally in the absence of external signals (Li, Nørrelkke and Cox, 2008) .

2 BACKGROUND

2.1 Ising model

The cellular Potts model is a generalization of a large-Q Potts model, which is itself a generalization of the Ising model. The Ising model, which was used in statistical physics to study ferromagnetism, was invented in 1920 by Wilhelm Lenz. This models helps to understand phase transition.

The model consists of a lattice populated by a discrete number of variables called 'spins', which can take one of two values 'up' or 'down', −1 or 1. Each node of the lattice is populated by a spin, and this spin may interact with its four nearest neighbors residing in the adjacent nodes. An energy function is defined,

$$E = -J \sum_{<k,l>} \sigma_i \, \sigma_j$$

The sum is over all pairs of neighbors. The parameter J is positive, and we shall take it equal to one. In a two-dimensional square lattice, the sites k and l then differ by either a lattice spacing in x or a lattice spacing in y. In a sum over pairs of neighbors, as in equation .we consider each pair only once, that is, we pick either <k,l> or <k,l> (Krauth, 2006).

As time is progressed spins will 'flip' in order to minimize this energy function. The CPM was introduced by Glazier and Graner in a 1992, in which they used an extended Potts model to simulate the sorting of biological cells in two-dimensions. Instead of two spins, there are N spins used in the CPM to represent N number of different biological cells. As well as, each spin is assigned to a certain cell type (Graner and Glazier, 1992).

2.2 Metropolis Algorithm

Monte Carlo methods is based on Markov chains is known as Markov Chain Monte Carlo. There are several MCMC algorithms. One of that algorithm is Metropolis algorithm. It is a widely use MCMC algorithm in statistical mechanics (Metropolis, 1953).

The Boltzmann distribution is a probability distribution or probability measure of the states in a system, which is found in statistical mechanics, mathematics and other sciences. The Metropolis algorithm is a strategy for obtaining a random sample from a Boltzmann distribution, which has also been generalized to obtain a random sample from any distribution which is proportional to the Boltzmann distribution. This is relevant because the Hamiltonian of both the CPM and Ising model are both proportional to the Boltzmann distribution, thus the Metropolis algorithm is useful for finding the minimum energy states for these two models.

2.3 Related works

There are lot of related works regarding to this project. Those are in different aspects such as computer simulations (Guisoni, Mazzitello and Diambra, 2018), statistical analysis (Wu, Giri and Wirtz, 2015), mathematical models (Danuser, Allard and Mogilner, 2013) and real cell experiments (Li, Nørrelkke and Cox, 2008).

3 THEORY

3.1 Cellular Potts model

The CPM simulates a 2D squared lattice and discretizes continuous cells on it. Each of the N cells has a spin number σ ∈ {1, …, N} and a cell type τ (σ). .Each lattice position $\vec{x}$ has a spin σ ($\vec{x}$) representing cell σ, giving each cell multiple lattice sites. Every configuration of the cell lattice has a corresponding total energy represented by the Hamiltonian. In a step of the simulation a random lattice site $\vec{x}$ is selected and given a copy attempt of its spin number σ ($\vec{x}$) to a randomly selected neighbor $\vec{x}$'. The copy attempt is accepted or rejected depending on the change of the Hamiltonian. Monte Carlo Step is the number of copy attempts that is given by

Monte Carlo Step (MCS) = 16 × Number of lattice sites (Graner and Glazier, 1992)

The total energy of a configuration is represented by the Hamiltonian. The Hamiltonian H is for neighboring lattice sites $\vec{x}$ and $\vec{x}$' is given by

$$H = \sum_{\vec{x},\vec{x}\prime} J_{\tau(\sigma(\vec{x})),\tau(\sigma(\vec{x}\prime))}\left(1 - \delta_{\sigma(\vec{x}),\sigma(\vec{x}\prime)}\right) + H_{area} + H_{perimeter} \quad (1)$$

$$H_{area} = \sum_{\sigma} \lambda(a_{\sigma} - A_{\tau(\sigma)})^2$$

$$H_{perimeter} = \sum_{\sigma} \mu(p_{\sigma} - P_{\tau(\sigma)})^2$$

Where $J_{\tau(\sigma(\vec{x})),\tau(\sigma(\vec{x}\prime))}$ represents the adhesion energy between two cell types, λ, μ are Lagrange multiplier specifying the strength of the area and perimeter constraint. a_{σ} And $A_{\tau(\sigma)}$ are the current and target cell area and p_{σ} and P_{σ} .The Kronecker delta is given by

$$\delta_{\sigma(\vec{x}),\sigma(\vec{x}\prime)} = \begin{cases} 1 & \sigma(\vec{x}) = \sigma(\vec{x}') \\ 0 & \sigma(\vec{x}) \neq \sigma(\vec{x}') \end{cases}$$

Setting the bond energy for the same spin zero and giving cells only a surface energy at their boundaries. A spin copy attempt $\sigma(\vec{x}) \rightarrow \sigma(\vec{x}')$ at temperature $T > 0$ is accepted with probability

$$P(\Delta H) = \begin{cases} e^{-\Delta H/T} & \Delta H > 0 \\ 1 & \Delta H \leq 0 \end{cases}$$

Calculating the change in Hamiltonian is easy and does not require the total Hamiltonian. It only involves the energy terms for the selected lattice site and its neighbors.

3.2 Simulation of active cell movement

Hamiltonian in cellular Potts model is insufficient to describe active cell movement. Therefore In order to simulate the active cell movement we consider an additional term in the Hamiltonian.

$$\Delta H = \Delta H_0 + \sum_\sigma F_\sigma . \Delta \vec{r}_\sigma$$

Where ΔH_0 is the change of energy due to Equation (1) and $\Delta \vec{r}_\sigma$ represents the displacement of the center of cell σ.

The strength of driving force $F = |F_\sigma|$ and a direction denoted by θ_σ. Strength is equal for all cells and constant over time. The driving force direction is different for each cell and evolves independently of the others.

θ_σ is actualized according to the following first-order autoregressive process:

$$\theta_\sigma(t^*) = \Phi\theta_\sigma(t^* - 1) + \Delta\theta\varepsilon(t^*)$$

Where t^* refers to the time of actualization of θ_σ, which is different from the Monte Carlo time step (MCS). Φ And $\Delta\theta$ are constant parameters, that can take values between (0, 1) and (0, π), respectively. ε (t) is a white noise with zero mean and unit variance (Guisoni, Mazzitello and Diambra, 2018).

4 METHODOLOGY

The implementation of active cell movement was done by MATLAB.

4.1 Simulation detail

In this project, we used Square lattice of size 256 × 256 sites. For all simulations in this project, we used periodic boundary conditions. The initial configuration is generated by partitioning the lattice into equal-sized square domains, corresponding to the cells, each cell containing 16 × 16 lattice sites. The squares alternate offsets in every other row, so the pattern resembles a brick wall arranged in common bond. It is assigned the same spin value to a number of randomly chosen cells, $\sigma = 0$ associated with the medium. Thus, the zero spin domain represents the medium. It is established the equivalence μm =pixel. Eukaryotic animal cells dimensions are considered as scaling. Since it is considered Eukaryotic animal cells, only involve single type of cells in this simulation. Therefore $\tau(\sigma)$ values are not important.

Simulations start with a given cell density ρ. Simulation is implemented at low density cell culture ($\rho = 0.2$) and high density cell culture ($\rho = 0.9$). Thermalization phase is implemented to allow dynamics to obtain adequate cellular shapes, during which no motility forces are applied on cells. 100 MCS is used in thermalization process. Once the system thermalizes, we establish the starting time $t = 0$. At this point the dynamics starts (Guisoni, Mazzitello and Diambra, 2018).

Parameters	Description	Value	Reference
$J_{\text{cell}-\text{cell}}$	cell–cell adhesive energy	2.0	estimated
$J_{\text{cell}-\text{medium}}$	cell–medium adhesive energy	1.0	estimated
λ	area elasticity	1.0	(Graner and Glazier, 1992)
$A_{\tau(\sigma)}$	Target area for cell type τ	π×64	(Guisoni, Mazzitello and Diambra, 2018)
μ	Perimeter elasticity	0.2	
$P_{\tau(\sigma)}$	Target perimeter for cell type τ	π×16	
F	Driving force	10.0	
$\Delta\theta$		π /3	
T	Temperature	2.0	(Graner and Glazier, 1992)

Table 1 Summary of the parameters used in the CPM simulations

As cells to stick together, it should be chosen $J_{cell-cell} > J_{cell-medium}$ in simulation.

4.2 Adhesion Energy

4.2.1 Choice of neighbourhood

Coupling neighborhood N_c is used in the calculation of the boundary energy, but does not play any role in the local connectivity test. Taking a large domain N_c for reduces the lattice anisotropy, but increases the number and range of interactions, thereby slightly increasing simulation time. Neighborhoods made of the 8 first neighboring sites (order II, or Moore neighborhood, Fig. 4.2.1.2) and 20 first neighboring sites (order IV neighborhood, Fig. 4.2.1.4) are commonly used (Durand and Guesnet, 2016).

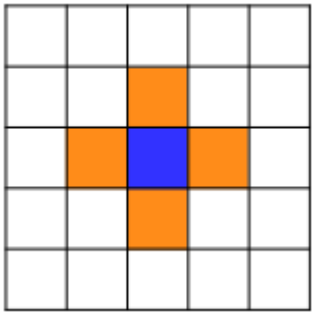

Figure 4-1 order I (or Von Neumann)

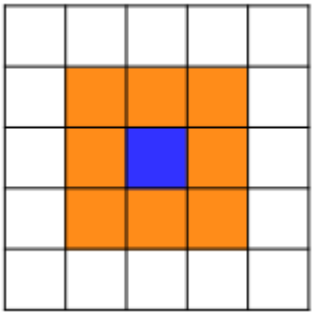

Figure 4-2 order II (or Moore) neighbourhood

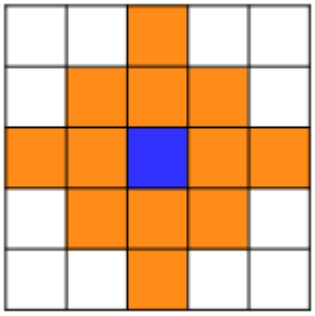

Figure 4-3 order III neighbourhood

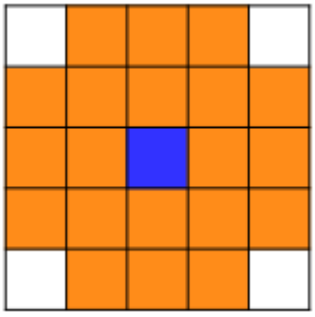

Figure 4-4 order IV neighbourhood.

Figure 4.2.1: : Different choices for the neighborhood (in orange) of the central site (in blue), in the square lattice: fig 4.2.1.1 order I (or Von Neumann) neighborhood; fig 4.2.1.2 order II (or Moore) neighborhood; fig 4.2.1.3 order III neighborhood; fig 4.2.1.4 order IV neighborhood

‘

4.2.2 Determine adhesion energy

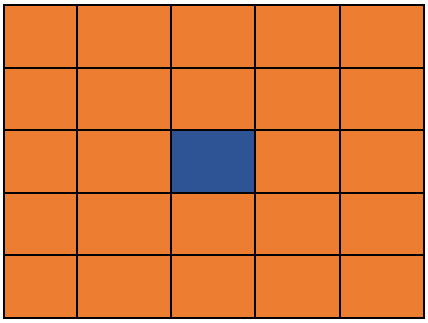

Figure 4-5 order V or extended Moore neighbourhood

(Fonstad, 2006)

Here 5th order neighbour is chosen. Which contribute to the energy $J_{\sigma_i \sigma_j}$ with weights proportional to the inverse of their distances $d_{i,j}$. If $\sigma_i \neq \sigma_j \neq 0$, the surface energy $J_{\sigma_i \sigma_j} = J_{\text{cell-cell}}/d_{i,j}$ where $J_{\text{cell-cell}}$ is the cell-cell adhesion constant. Otherwise if one of the neighbouring sites, i or j belongs to the medium, the surface energy is given by $J_{\sigma_i \sigma_j} = J_{\text{cell-medium}}/d_{i,j}$, where $J_{\text{cell-medium}}/d_{i,j}$ is cell – medium adhesion constant(Guisoni, Mazzitello and Diambra, 2018).

4.3 Area energy

Suppose we have the following situation, and we are looking at element x is coloured blue. The randomly selected neighbour of x is coloured red.

X	X	X	Y
X	X	Y	Y
X	Y	Y	Y

Figure 4-6

After the copy Y into X

X	X	X	Y
X	Y	Y	Y
X	Y	Y	Y

Figure 4-7

In this transition only change one unit of area.

If X > 0

$$\Delta H_{area} = \lambda\left((a_x - 1) - A_{\tau(x)}\right)^2 - \lambda(a_x - A_{\tau(x)})^2$$

$$= \lambda\,(-2a_x + 2A_{\tau(x)} - 1)$$

If Y > 0

$$H_{area} = \lambda((a_y + 1) - A_{\tau(y)})^2 - \lambda(a_y - A_{\tau(y)})^2$$

$$= \lambda\,(2a_x - 2A_{\tau(x)} + 1)$$

4.4 Perimeter energy

First, lattice is converted into binary image while pixels corresponding to relevant cell equal to 1 and otherwise equal to 0.

Suppose we have binary image relevant to specific region

0	0	0	0	0	0	0	0
0	1	1	1	1	1	1	0
0	0	1	1	1	1	0	0
0	0	1	1	1	0	0	0
0	0	1	1	1	0	0	0
0	0	1	1	1	0	0	0
0	0	1	1	1	0	0	0
0	0	0	0	0	0	0	0

Figure 4-8 binary image of the specific region

Count edges that a single edge pixel has and locate edge count in that pixel

0	0	0	0	0	0	0	0
0	3	1	1	1	1	3	0
0	0	1	0	1	2	0	0
0	0	1	0	1	0	0	0
0	0	1	0	1	0	0	0
0	0	1	0	1	0	0	0
0	0	2	1	2	0	0	0
0	0	0	0	0	0	0	0

Figure 4-9 processed image that count edges and locate in edge pixel

Finally take sum over each lattice sites in the system. That sum is the parameter of the relevant object.

4.5 Cell centroid

In order to find energy difference of term $\sum_\sigma F_\sigma . \Delta\vec{r}_\sigma$. It is essential to find centroid of the cell. Here it assumed mass of cell ∞ Area of the cell.

First we convert lattice into binary image while pixels corresponding to relevant cell equal to 1 and otherwise equal to 0. Using regionprops and bwconncomp functions in MATLAB.it is possible to find Areas and Centroids of objects in the binary image. Here it essential to consider lattice with periodic boundary condition. It should be possible to calculate center of mass even that cell locate in the boundary area. Hereafter each region in the lattice considers as particle.

4.5.1 Systems with periodic boundary conditions

A generalized method for calculating the center of mass for periodic systems is to treat each coordinate, *x* and *y* and/or *z*, as if it were on a circle instead of a line. The calculation takes every particle's *x* coordinate and maps it to an angle (Bai and Breen, 2008),

$$\theta_i = (\frac{x_i}{x_{\max.}})\times 2\pi$$

$x_{\max.}$ is the lattice size in the x direction and $x_i \in [0, x_{\max.})$. From this angle, two new points (ξ_i, ζ_i) can be obtained.

$$\xi_i = \cos(\theta_i)$$

$$\zeta_i = \sin(\theta_i)$$

In the (ξ, ζ) plane, these coordinates lies on a circle of radius 1. From the collection of ξ_i and ζ_i values from all the particles. The averages $\bar{\xi}$ and $\bar{\zeta}$ are calculated.

$$\bar{\xi} = \frac{1}{M}\sum_{i=1}^{n} m_i \xi_i$$

$$\bar{\zeta} = \frac{1}{M}\sum_{i=1}^{n} m_i \zeta_i$$

$$M = \sum_{i=1}^{n} m_i$$

These values are mapped back into a new angle, $\bar{\theta}$ from which the *x* coordinate of the center of mass can be obtained:

$$\bar{\theta} = atan2\left(-\bar{\zeta}, -\bar{\xi}\right) + \pi$$

$$x_{centre\ of\ mass} = x_{max}\frac{\bar{\theta}}{2\pi}$$

The process can be repeated for all dimensions of the system to determine the complete center of mass.

5 RESULTS AND ANALYSIS

5.1 Cell displacement

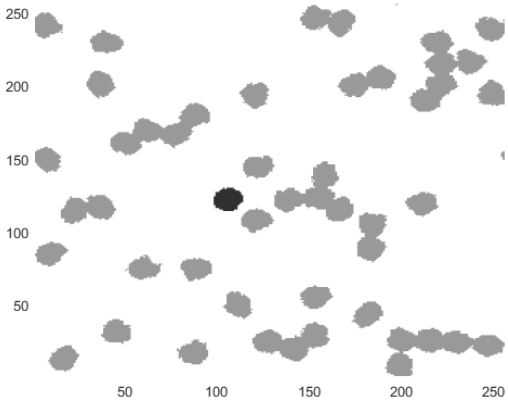

Figure 5-1 initial time t = 0 MCS with presence of driving force acting on each cell

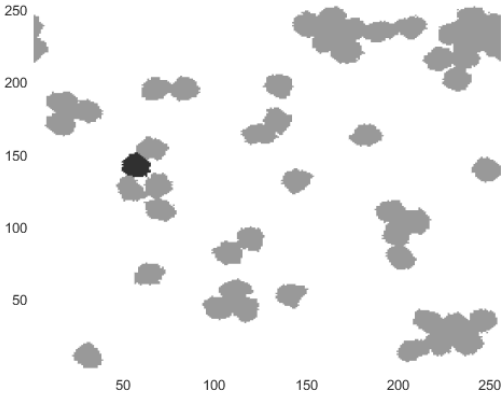

Figure 5-2 after t = 500 MCS

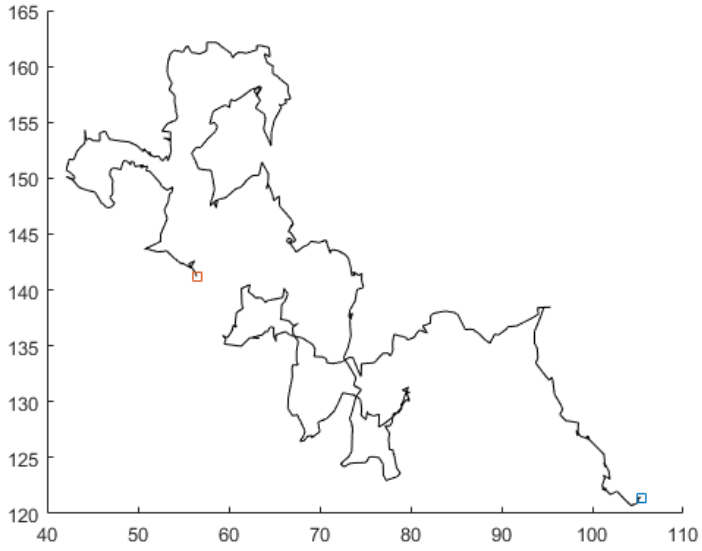

Figure 5-3 trajectory of the black coloured cell

Above results are taken by using 256×256 lattice during 500 MCS. In above trajectory (figure 5-3), start point of the trajectory at t = 0 MCS is represented by blue square shape marker and end point of the trajectory at t = 500 MCS is represented by red square shape marker. Here cell trajectory is defined as positions of a cell at different time points over the course of time *t* of observation. Usually, the time step between successive cell positions is a constant expressed in units of MCS. This trajectory resembles those traced by Dictyostelium cells (Li, Nørrelkke and Cox, 2008). . Here black colored cell (figure 5-1, figure 5-2) has displaced across scales much larger than the cell size. Persistent movement happens because of driving force that has a constant strength and is applied with constant direction during a mean time τ.

5.2 Velocity distribution

Displacement of the cell *i* is defined as $\Delta\vec{r_i} = \overrightarrow{r_i\,(t\,+\,\Delta t)} - \overrightarrow{r_i(t)}$ in a time interval Δt. mean velocity $\overrightarrow{v_i} = \frac{\Delta\vec{r}_i}{\Delta t}$.

When density of cell culture ρ = 0.2 and Δt = 1,

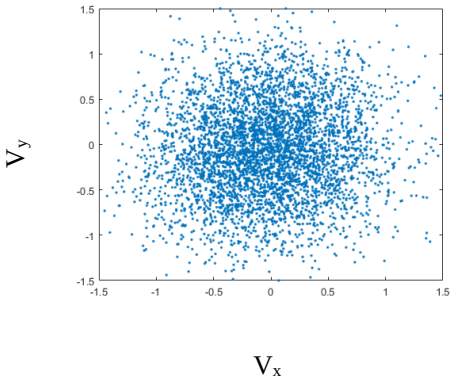

Figure 5-4 Cell velocities Vx vs V_y

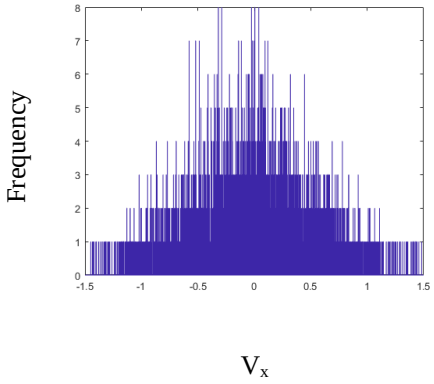

Figure 5-5 Cell velocities histogram of Vx

When density of cell culture ρ = 0.9 and Δt = 1,

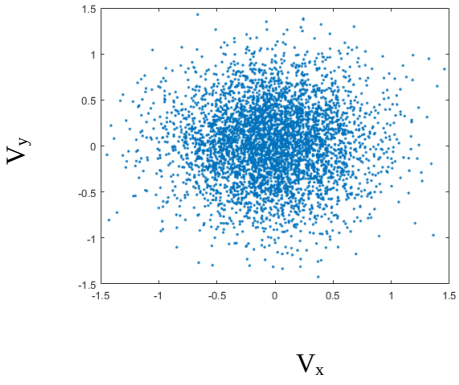

Figure 5-6 Cell velocities Vx vs Vy

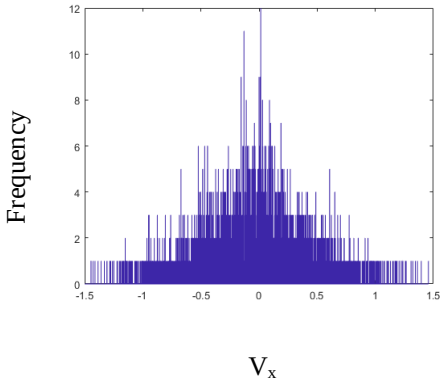

Figure 5-7 Cell velocities histogram of Vx

Above results are taken by using 128×128 lattice during 500 MCS. These distributions were obtained by tracking all 9 cells in low density and 9 out of 49 cells chosen random in high density. For Δt = 1, the velocity distributions for both densities are similar, resembles Gaussian distributions.

5.3 Displacement angle

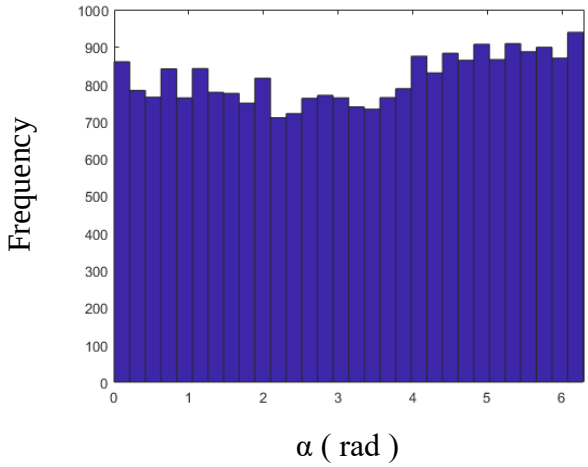

Figure 5-8 Frequency distribution of cell displacement angle α during 500 MCS

Here 256×256 size of lattice were used. Cell displacement angle α was considered by using Δt = 1. This histogram was computed over all cells during a simulation in low density cell culture. This histogram illustrate approximately uniform distribution. It means each and every angle have equal probability of occurrence.

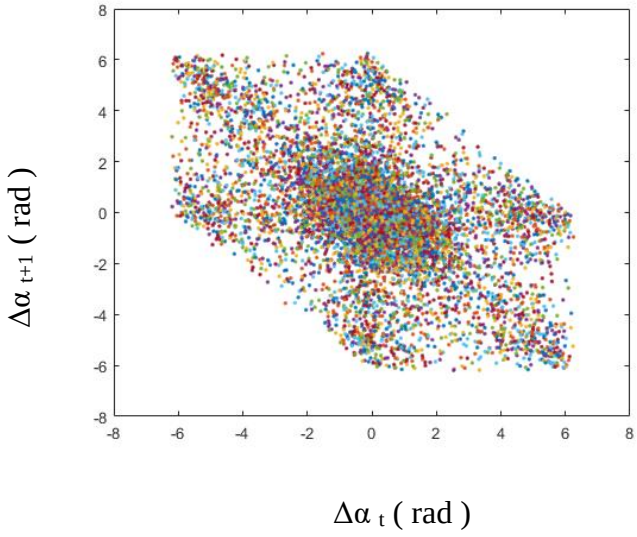

Figure 5-9 $\Delta\alpha_t$ versus $\Delta\alpha_{t+1}$

Here 256×256 size of lattice were used and plot only for low density culture.it illustrate negative relationship.

5.4 Mean square displacements

Mean square density calculated as $MSD(t) = < (\overrightarrow{r_i(t)} - \overrightarrow{r_i(0)})^2 >$

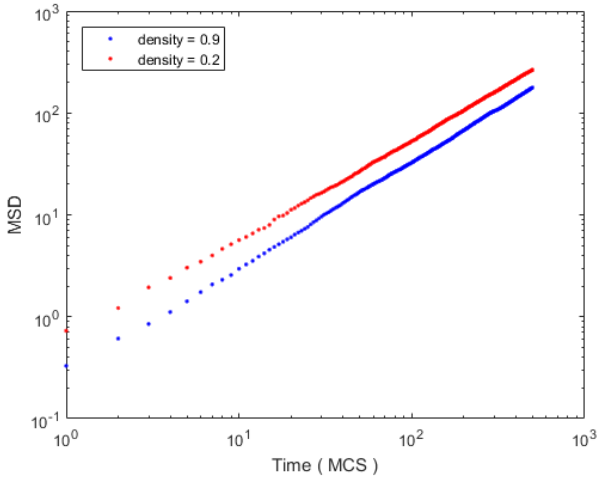

Figure 5-10 MSD in high and low densities

The MSD obtained for high density is lower than that obtained for low density, as expected.

6 DISCUSSION

In this project, positions of each cell centroids was collected for each MCS throughout entire simulation time. Using those positions, statistical analysis was carried out to discover dynamics of the cells in absence of external signal. This experiment have done for both high and low density cell cultures. Lattice of size 256×256 were used to discover trajectories of the cells, resultant displacement of the cells during 500 MCS and displacement angles in low density cell culture. Since simulation in lattice of size 256×256 for high density cell culture was extremely slow, lattice of size 128×128 were used to find velocity distribution and MDS for both low and high density cell cultures. In here, Periodic boundary conditions are used to approximate large system by using small part of the system. Then by using this small part, it is possible to measure characteristics of the large system.

Here, individual cell trajectories were considered to evaluate the displacement behaviour of the individual cells in this model. These trajectories resemble those traced by Dictyostelium cells (Li, Nørrelkke and Cox, 2008),which travel much longer distances than the typical cell size. Persistent and random walk of the cell can be seen in **Figure 6-1.** Persistent walk means walker is more likely to move in the same or a similar direction to its previous movement direction. This tendency to continue in the same direction is known as persistence. Persistent movement in our simulation is due to the driving force that has a constant magnitude and is applied with constant direction during a mean time τ.

Velocity distributions of the cells is also very essentials in this simulation. Here, both high and low density cell cultures were used to compare velocity distributions. For $\Delta t = 1$, the velocity distributions for both densities are similar with Gaussian distributions. This result acceptable with real cell experiment(Li, Nørrelkke and Cox, 2008). More values for Δt couldn't obtain velocity distribution because of insufficient data.

Cell frequency distribution of angle displacement was also obtained. According to histogram (**Figure 6-8)**, cells can move in any direction with equal probabilities. Therefore, there is not a preferential direction for each cell in low density cell culture.

Displacement angle correlation is also important statistical parameter to discover new model. **Figure 6-2** illustrate more negative relationship Therefore, this plot shows that two consecutive angles of displacement are anti-correlated. This characteristic of cell motion has also been observed in experiments with Dictyostelium cells (Li, Nørrelkke and Cox, 2008). Here, simulation was not implemented for high density cell culture because of insufficient data.

Mean square displacement is the most common measure of random cell movements. Behavior of MSD with time is expected for both densities. The MSD obtained for high density is lower than that obtained for low density, as also expected. Because of more interactions of cells in high density than low density.

This simulation was programmed by MATLAB. But it is very high level language. Therefore it takes much more time to complete simulation. Therefore it is very difficult to debugging the program. It is most suitable to use C / C++ like relative low level language. Therefore using MATLAB is the main drawback of this project.

According to results and analysis, there are features that are acceptable with real cell experiments and theoretically. But above features are not enough for modelling of cell migration in absence of external signal. Therefore it should be use more statistical quantities to models and get deep insight about active cell movement.

7 CONCLUSION

Steinberg experiments has been explained that differential adhesion is a main factor for cell sorting and related cell rearrangement(Steinberg, 1963; Foty and Steinberg, 2005) . Graner and Glazier have shown that the CPM model with differential adhesion, as driving force, is able to implement cell sorting (Graner and Glazier, 1992). Here two stochastic processes are used in this simulation. One is metropolis algorithm that use as update method of lattice sites. Another one is autoregressive function that governs dynamics of cell movement direction.

In this project, several statistical features were considered to evaluate the model. Some features were agreed with real cell experiments and some features were agreed with theoretical expectations. Especially persistent random motion was demonstrated in low density cell culture and it's accepted with real cell experiments (Li, Nørrelkke and Cox, 2008). Here simulation was done for low and high densities. Then results are compared for effects of two different level of cell interactions. Velocity distributions are same for both densities for $\Delta t = 1$ not regarding densities of the cell cultures.

In future works, interesting considerations are the extension to 3D and the use of a six-connected neighbourhood on a hexagonal grid instead of an eight-connected (Moore) neighbourhood on rectangular grid.

On the technical side, there are two options for improve performance of the simulation. Non–Metropolis Monte Carlo algorithms of rejection free dynamics such as the N-fold Way and the kinetic Monte Carlo approach is one option. Because of too low acceptance probabilities of spin flips often waste a lot of calculation time. Other widely use option is distributing computing(Chen *et al.*, 2007; Tapia and D'Souza, 2011).

8 REFERENCES

Bai, L. and Breen, D. (2008) 'Calculating Center of Mass in an Unbounded 2D Environment', *Journal of Graphics Tools*, 13(4), pp. 53–60. doi: 10.1080/2151237X.2008.10129266.

Chen, N., Glazier, J. a., Izaguirre, J. a., & Alber, M. S. (2007). A parallel implementation of the Cellular Potts Model for simulation of cell-based morphogen', *Computer Physics Communications*, 176(11–12), pp. 670–681. doi: 10.1016/j.cpc.2007.03.007.

Danuser, G., Allard, J. and Mogilner, A. (2013) 'Mathematical Modeling of Eukaryotic Cell Migration: Insights Beyond Experiments', *Annual Review of Cell and Developmental Biology*, 29(1), pp. 501–528. doi: 10.1146/annurev-cellbio-101512-122308.

Durand, M. and Guesnet, E. (2016) 'An efficient Cellular Potts Model algorithm that forbids cell fragmentation', *Computer Physics Communications*, 208(1), pp. 54–63. doi: 10.1016/j.cpc.2016.07.030.

Fonstad, M. A. (2006) 'Cellular automata as analysis and synthesis engines at the geomorphology-ecology interface', *Geomorphology*, 77(3–4), pp. 217–234. doi: 10.1016/j.geomorph.2006.01.006.

Foty, R. A. and Steinberg, M. S. (2005) 'The differential adhesion hypothesis: A direct evaluation', *Developmental Biology*, 278(1), pp. 255–263. doi: 10.1016/j.ydbio.2004.11.012.

Graner, F. and Glazier, J. A. (1992) 'Simulation of biological cell sorting using a two-dimensional extended Potts model', *Physical Review Letters*, 69(13), pp. 2013–2016.

Guisoni, N., Mazzitello, K. I. and Diambra, L. (2018) 'Modeling Active Cell Movement With the Potts Model', *Frontiers in Physics*, 6(June), p. 61. doi: 10.3389/fphy.2018.00061.

Hester, S. D. *et al.* (2011) 'A multi-cell, multi-scale model of vertebrate segmentation and somite formation', *PLoS Computational Biology*, 7(10). doi: 10.1371/journal.pcbi.1002155.

Jagt, J. W. M., Neumann, C. and Schulp, A. S. (2007) 'Bioimmuring late Cretaceous and Recent oysters: "A view from within"', *Geologica Belgica*, 10(1–2), pp. 121–126. doi: 10.1016/J.CUB.2003.09.014.

krauth, W. (2006) *Statistical Mechanics: Algorithms and Computations*.

Li, L., Nørrelkke, S. F. and Cox, E. C. (2008) 'Persistent cell motion in the absence of external signals: A search strategy for eukaryotic cells', *PLoS ONE*, 3(5). doi: 10.1371/journal.pone.0002093.

Mak, M. *et al.* (2016) 'Single-Cell Migration in Complex Microenvironments: Mechanics and Signaling Dynamics', *Journal of Biomechanical Engineering*, 138(2), p. 021004. doi: 10.1115/1.4032188.

Merks, R. M. H. *et al.* (2008) 'Contact-inhibited chemotaxis in de novo and sprouting blood-vessel growth', *PLoS Computational Biology*, 4(9). doi: 10.1371/journal.pcbi.1000163.

Metropolis, N. (1953) 'Metropolis-Et-Al-1953', *The Journal of chemical physicsh*, p. 1087. doi: 10.1111/maps.12421.
"
Scianna, M. (2015) 'An extended Cellular Potts Model analyzing a wound healing assay', *Computers in Biology and Medicine*, 62, pp. 33–54. doi: 10.1016/j.compbiomed.2015.04.009.

Scianna, M. and Preziosi, L. (2012) 'Multiscale Developments of the Cellular Potts Model', *Multiscale Modeling & Simulation*, 10(2), pp. 342–382. doi: 10.1137/100812951.

Steinberg, M. S. (1963) 'Reconstruction of tissues by dissociated cells', *Science Science*, 141(3579), pp. 401–408. doi: 10.1126/science.141.3579.401.

Steinberg, M. S. (1975) 'Adhesion-guided multicellular assembly: a commentary upon the postulates, real and imagined, of the differential adhesion hypothesis, with special attention to computer simulations of cell sorting', *Journal of Theoretical Biology*, 55(2), pp. 431–443. doi: 10.1016/S0022-5193(75)80091-9.

Szabó, A. *et al.* (2010) 'Collective cell motion in endothelial monolayers', *Physical Biology*, 7(4). doi: 10.1088/1478-3975/7/4/046007.

Szabó, A. and Merks, R. M. H. (2013) 'Cellular Potts Modeling of Tumor Growth, Tumor Invasion, and Tumor Evolution', *Frontiers in Oncology*, 3(April), pp. 1–13. doi: 10.3389/fonc.2013.00087.

Tapia, J. J. and D'Souza, R. M. (2011) 'Parallelizing the Cellular Potts Model on graphics processing units', *Computer Physics Communications*. Elsevier B.V., 182(4), pp. 857–865. doi: 10.1016/j.cpc.2010.12.011.

Wu, P. H., Giri, A. and Wirtz, D. (2015) 'Statistical analysis of cell migration in 3D using the anisotropic persistent random walk model', *Nature Protocols*. Nature Publishing Group, 10(3), pp. 517–527. doi: 10.1038/nprot.2015.030.

APPENDIX